Materials for life sciences

Warp-knitted fabric structures for a novel biomimetic artificial intervertebral disc for the cervical spine

Celien A. M. Jacobs[1] (iD), Abdelrahman M. Abdelgawad[2,4], Stefan Jockenhoevel[2,3], Keita Ito[1], and Samaneh Ghazanfari[2,3,*]

[1] *Orthopedic Biomechanics, Department of Biomedical Engineering, Eindhoven University of Technology, De Rondom 70, 5612 AP Eindhoven, The Netherlands*

[2] *Faculty of Science and Engineering, Aachen-Maastricht Institute for Biobased Materials, Maastricht University, Brightlands Chemelot Campus, Urmonderbaan, 226167 RD Geleen, The Netherlands*

[3] *Department of Biohybrid and Medical Textiles (BioTex), AME – Institute of Applied Medical Engineering, Helmholtz Institute, RWTH Aachen University, Forckenbeckstraβe 55, 52074 Aachen, Germany*

[4] *Textile Engineering Chemistry and Science Department, Wilson College of Textiles, North Carolina State University, Raleigh, NC, USA*

ABSTRACT

As an attempt to better replicate the complex kinematics of a natural disc, a novel biomimetic artificial intervertebral disc replacement (bioAID) has been developed containing a swelling hydrogel core as nucleus pulposus, a fiber jacket as annulus fibrosus and metal endplates to connect the device to the adjacent vertebrae. The first prototype consisted of a weft-knitted fiber jacket, in which only a single fiber was used to create the jacket structure. This can endanger the structural integrity of the complete device upon yarn damage. Therefore, in this study, several warp-knitted textile structures were assessed to (1) ensure structural integrity, (2) while allowing for swelling constraint of the hydrogel and (3) behaving as one integrated unit similar to the natural IVD. Moreover, the fiber jacket should (4) act as a scaffold that allows bone ingrowth to ensure long-term stability and (5) have a good durability, (6) be wear resistant and (7) have good manufacturing feasibility with good quality control. In this study, 4 different stitch patterns, including 2 × 1 and 1 × 1 lapping with and without a pillar stitch, were produced. The effect of the stitch pattern and stitch density on the fabric mechanical properties and device swelling and compressive strength was assessed. As a next step, the effect of using multiple layers of fabrics, mimicking the layered structure of annulus fibrosus, on the functional

---

Celien A. M. Jacobs and Abdelrahman M. Abdelgawad both shared first authorship of this article.

Handling Editor: Stephen Eichhorn.

Address correspondence to E-mail: Samaneh.ghazanfari@maastrichtuniversity.nl
E-mail Addresses: c.a.m.jacobs@tue.nl; Aabdelgawad2@gmail.com; stefan.jockenhovel@maastrichtuniversity.nl; jockenhoevel@ame.rwth-aachen.de; k.ito@tue.nl

capacity of the bioAID was characterized. All textile structures were capable of limiting the swelling of the hydrogel while withstanding its internal pressure and showing sufficient wear resistance. However, only the 2 × 1 and 2 × 1 with pillar stitch had a pore size range that was suitable for cell infiltration to facilitate osseointegration as well as having the highest strength of the complete device to ensure safety under compression loading. Incorporating different number of jacket layers of these two stitch patterns did not show any significant effect. When also taking the structural parameters into consideration, the 2 × 1 lapping design with 4 layers was able to constrain hydrogel swelling, provide a high compressive strength, could facilitate cell infiltration and had dimensions within the range of a natural intervertebral disc.

Introduction

Neck pain is a persistent problem that affects millions of people nowadays, mainly caused by spinal disorders affecting intervertebral discs (IVD) [1]. The most common surgical practice to treat severely diseased IVDs is anterior cervical discectomy and fusion (ACDF), where after removal of the dysfunctional IVD, the vertebrae are fused with new bone growth to resolve the pain by restoring the disc height and blocking the motion. However, occurrence of adjacent segment diseases due to the loss of motion urged the development of cervical total disc replacements (CDRs) where the diseased natural disc is replaced with a motion preserving prosthesis. First-generation designs were based on the ball-and-socket principle, which consists of the superposition of solid plates and a core to provide motion based on articulation. The axial properties of such devices are rigid, providing little compression absorption while the natural IVD is an osmotic, viscoelastic body, showing hysteresis and time-dependent deformation [2]. Several clinical trials showed that the implantation of such CDR devices altered the natural motion pattern, caused facet joint overloading, and increased the risk of adjacent segment disease [3, 4].

Therefore, second-generation artificial intervertebral discs (AIDs) that can mimic the viscoelastic behavior of a natural disc have been developed in recent years. These devices provide motion from deformable components, allowing motion in all six degrees of freedom and combined motions [5, 6]. One of those devices is the biomimetic artificial intervertebral disc (bioAID) introduced by Peter van den Broek et al. (2012), which based on an FEM study has shown to replicate natural disc kinematics [6]. The bioAID device contains a hydrogel core mimicking the natural swelling nucleus pulposus, a textile fiber jacket as the tensile load-bearing annulus fibrosis, and a titanium endplate to secure the device to the adjacent vertebrae (Fig. 1).

One of the key components in the fiber jacket is the medical-grade ultrahigh-molecular-weight-polyethylene (UHMWPE) fiber, tradename Dyneema Purity® (DSM Biomedical, Geleen, the Netherlands), which encloses the hydrogel core to imitate the nonlinear viscoelastic behavior and osmotic prestress of the natural IVD. Dyneema Purity® fiber has exceptionally long and oriented molecular chains that can withstand and distribute high loads effectively. In addition, the fiber exhibits high abrasion and cut resistance and inert chemical properties [7]. Therefore, the bioAID is assumed to possess the required strength, stability and shock absorbance capacity while allowing a semi-constrained motion based on deformation.

The first design of Peter van den Broek et al. (2012) was developed for the lumbar region of the spine [6]. However, clinical need, market size, interest of industry and clinicians revealed more opportunities for the cervical spine. Moreover, the fiber jacket of this first prototype was a weft-knitted stocking fabricated from a single Dyneema Purity® yarn [8]. The jacket showed no failure up to 15kN (30–35% strain) static compression and remained intact after 10 million cycles of axial loading between 600 – 6000 N; however, the structure safety and integrity are of concern as the yarn could be cut or damaged, e.g., during device implantation.

Unlike weft-knitting, warp-knitted structures are made from several yarns, which makes them more
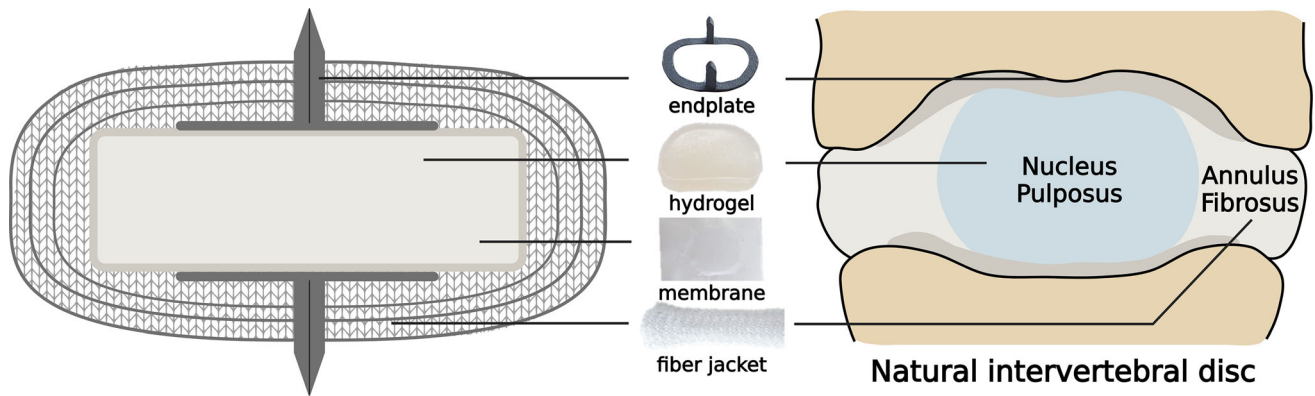
Figure 1 Schematic representation of the bioAID and its biomimicry compared to a natural disc.

resistant to failure [9]. In comparison with weft-knitted structures, warp-knitted ones are typically less elastic, which leads to a better swelling and range of motion constraint function of the fiber jacket. Therefore, in this study, several warp-knitted textile patterns were mechanically and structurally assessed and optimized to fit the cervical intervertebral space. More specifically, the biomechanical objectives of the fiber jacket are 1) ensuring structural integrity, 2) while allowing for swelling constraint of the hydrogel and 3) behaving as one integrated unit similar to the natural IVD. Moreover, the fiber jacket should 4) act as a scaffold that allows bone ingrowth to ensure long-term stability and 5) have a good durability, 6) be wear resistant and 7) have good manufacturing feasibility with good quality control.

Materials and methods

Hydrogel preparation

The hydrogel was produced by dissolving sodium methacrylate (monomer, 0.02 mol ratio), 2-hydroxyethyl methacrylate (monomer, 0.18 mol ratio), poly (ethylene glycol) dimethacrylate (cross-linker, 0.00001 mol ratio), $2 \times 2'$ azobis (2-methylpropionamidine) dihydrochloride (initiator, 0.001 mol ratio) in distilled water (all analytical grade, Sigma-Aldrich, Zwijndrecht, the Netherlands). This hydrogel solution was then poured onto a disc of polyurethane foam (Ø 10×0.2 cm, MCF.03, Corpura B.V., Etten-Leur, The Netherlands) that soaked up the solution, after which it was exposed to UV light (UVP XX15L, 365 nm, Analytik Jena, Upland, CA USA) for two hours at room temperature in ambient air. To complete the polymerization, it was submerged in a 45 °C water bath for 14 h. Next, the hydrogels were punched out in kidney shape of $21 \times 14.5 \times 2$ mm or $14 \times 13 \times 2$ mm, being the human and canine dimensions, respectively.

Fiber jacket fabrication

The production of the tubular warp-knitted jackets was performed on a double-face Raschel machine with Jacquard unit of type DJ 6/2 EL (Karl Mayer Textilmaschinenfabrik GmbH, Obertshausen, Germany) with a machine gauge of E32 at a speed of 60 rpm. First, the UHMWPE yarn was rewound from the parent bobbin to suitable bobbins for the creel of the warp-knitting machine. Next, to identify optimal design properties of the fiber jacket and achieve a stable manufacturing process, several experiments were executed (Table 1). In the first experiment, the effect of 4 different fabric structures (Fig. 2, lapping design being 2×1, 1×1, 2×1 + open pillar stitch, and 1×1 + open pillar stitch) of 10 stitch/cm, on the biomechanical properties and assembly of the device was studied. In the second knitting experiment, a stitch density of 8 stitch/cm was used to facilitate usage of more commonly available textile machines (double-needle bed Rachel machine with gauge E20, Mini-tronic 800, RIUS-COMATEX, Barcelona, Spain). Based on the ease of assembly, structural characteristics, swelling and compression strength of experiment 1, only the 2×1 and 2×1 + pillar stitch lapping designs were used to determine the effect of the stitch density and amount of layers for optimal functioning of the bioAID (6, 5 or 4 layers for the 2×1 lapping design and 5, 4 or 3 layers for the 2×1 lapping with pillar stitch design)

Table 1 Experimental design to determine the optimal fiber jacket configuration

	Experiment 1: effect of stitch patterns	Experiment 2: effect of stitch density and layers
Density	10 stitch/cm	8 stitch/cm
Stitch pattern	1×1	2×1
	1×1 + pillar stitch	2×1 + pillar stitch
	2×1	
	2×1 + pillar stitch	
Read outs	Human device mechanical characterization	Canine device mechanical characterization
	Fabric mechanical and structural properties	Fabric mechanical and structural properties

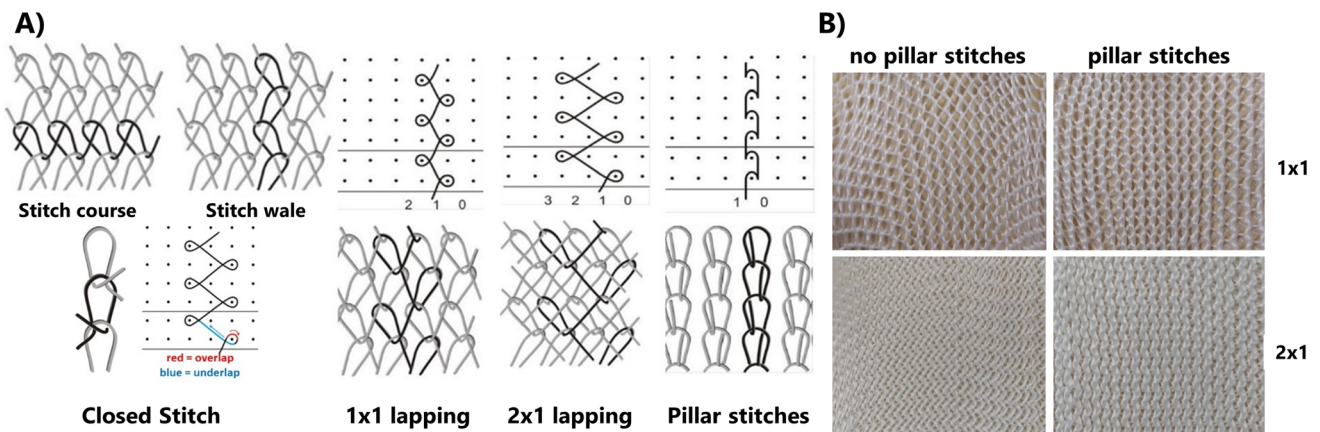**Figure 2** **a** Schematic drawing of stitch components and different stitch designs; **b** knitted tubes with different lapping designs (1×1, 1×1 + pillar stitches, 2×1, and 2×1 + pillar stitches).

to replicate the layered structure of the annulus fibrosus [10]. The diameter of the tubular fiber jackets was calculated to tightly fit around the hydrogel core and restrict swelling, resulting in a theoretical diameter of 18 mm. However, this diameter had to be adjusted for fabrics with different course stitch densities and lapping designs since this affects the elasticity of the fabric. Both fabric structures and complete assembled devices were mechanically assessed.

Device assembly

The device is composed of three parts, a hydrogel core, a fiber jacket and two endplates (Fig. 3), which are assembled to create human and canine prototypes [6]. Canine prototypes were evaluated as preparation for the planned animal trials. First of all, the hydrogel was wrapped in an UHMWPE membrane (38 μm thick, 5 g/m2, 0.9 μm pore, membrane, DSM Biomedical, Geleen, the Netherlands) and heat sealed using a thermal cutter (HSG-0, HSGM, Walluf,

Germany) to contain the hydrogel and prevent leaching of hydrogel particles. The hydrogel sealed in the membrane was then inserted inside the tubular warp-knitted fiber jacket made of multifilament UHMWPE yarn (Dyneema Purity® SGX, dtex110, TS 100, DSM Biomedical, Geleen, Netherlands). After the core was positioned at the bottom of the jacket such that it laid in the transverse plane of the tube, the open end was twisted tight, and the jacket was pulled backward, inside out, over the core again, closing the open side with a 180° twist, resulting in the first two jacket layers. The wrapping process was repeated until the number of desired layers was reached. At the innermost layer of the jacket layers, two wire-eroded titanium endplate rings (10 × 9 × 0.3 mm) with 2 mm pins, on either flat surface of the implant, was inserted before closing the jacket, such that the pins protruded out of the jacket. The open end of the jacket was closed by manual stitching using UHMWPE yarn (Dyneema Purity® SGX, dtex110, TS 100, DSM Biomedical, Geleen, Netherlands).
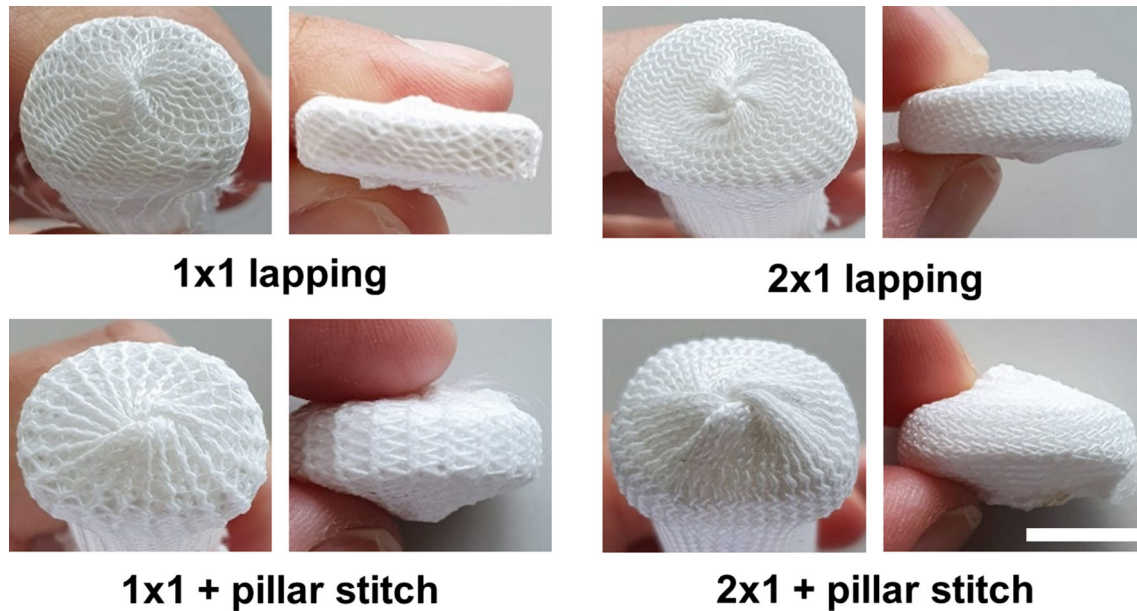
Figure 3 Images during the production procedure for each textile structures, showing the formation of the knot at the central cranial and caudal sides of the implant. Scale: 10 mm.

Fabric structural and mechanical evaluation

The fabric structures (1×1 (10 stitch/cm), 1×1 with pillar (10 stitch/cm), 2×1 (8 and 10 stitch/cm) and 2×1 with pillar stitch (8 and 10 stitch/cm) were characterized in terms of the fabric weight, thickness, porosity, bursting strength and abrasion resistance. Fabric weight (g/m2) was determined based on ASTM D3776, where the areal density (mass/unite area) was obtained by weighing 2×10 cm^2 samples and dividing it by the area ($n = 3$). Thickness (mm) measurements were executed following ASTM D1777-96. An automatic thickness gauge was used, where a specimen was placed on the base of a thickness gauge and a weighted presser foot applied a pressure of 0.41 Bar ($n = 3$). The porosity of the fabric was analyzed by microscopy using a magnification of 100x (Keyence Microscope VHX S550t, USA). Next, the images were binarized using ImageJ (NIH, USA) and used to calculate the pore size ($n = 3$, µm). Bursting strength was assessed as described in ASTM D3786/D3786M. Briefly, a compressive force was applied at a constant rate of 300 mm/min on the sample (12×12 mm) using a polished, hardened steel ball until rupture occurred (Autoburst SDL-Atlas M229, SDL Atlas Textile Testing Solutions, Rock Hill, USA). Displacement and load were continuously recorded and used to calculate the average failure load ($n = 5$). Lastly, abrasion resistance was measured, as reported in ASTM D4966-12, to assess the risk of wear debris. Three samples (circular, diameter = 38 mm) were preconditioned at 20 °C at relative humidity of 65% and rubbed against standard wool felt under 12 kPa pressure until two or more yarns were broken, or when a hole appeared (Martindale Wear and Abrasion Tester M235, SDL Atlas Textile Testing Solutions, Rock Hill, USA). The average number of rubs required to rupture two or more yarns or develop a hole in a knitted fabric was reported ($n = 4$).

Device evaluation: swelling and mechanical integrity

To assess what textile structure and number of jacket layers is optimal for the complete implant, in terms of swelling restriction and compressive mechanical strength, the swelling properties and compressive mechanical strength of the implants were evaluated. It was assumed that the incorporation of the endplate would not have a large effect on the swelling and compressive strength of the device and was therefore not included in the tested prototypes. Swelling capacity of the produced bioAID prototypes was tested in PBS (Dulbecco's Phosphate Buffered Saline, Sigma Aldrich) at 37 °C under a 50 N load to mimic the passive compressive load of a cervical spine [11, 12]. The mass was determined before the

experiment and after reaching swelling equilibrium and used to calculate the swelling mass ratio (Q) by Eq. (1), where Ms is the mass in the swollen state and Md is the mass in the dry state.

$$Q = \frac{M_s - M_d}{M_d} \qquad (1)$$

Compressive strength and mechanical integrity were determined by a static axial compression test. Samples were subjected to compressive load at 3 mm/min until failure or limit of the load cell (MTS; criterion model 42, MTS Systems corporation, Eden Prairie, MN USA, load cell of 1 kN). Failure was defined as a force drop at constant displacement. The strength was defined as the highest load before failure, or "higher than 5 kN" (limit of load cell), and stiffness was determined as the slope of the linear region of the curve. After testing, damage of fiber jacket was macroscopically inspected.

Statistical analysis

Mean and standard deviation were calculated using Microsoft Excel. Comparisons between experimental groups were determined by one-way ANOVA, followed by Tukey's honest post hoc analysis to assign significant differences. Normal distribution was verified using Shapiro–Wilk test and homogeneity of variance by Bartlett's test. If the experimental groups did not show homogeneity of variances or normal distribution, a nonparametric Kruskal–Wallis with Dunn's multiple comparison tests was performed. A $p < 0.5$ was considered as a statistically significant difference. All statistical comparisons between groups were performed using GraphPad Prism version 8.02 for Windows (GraphPad Software).

Results

Fabric structural properties

As expected, fabric thickness and fabric weight were lower for the 1 × 1 lapping design compared to the 2 × 1 lapping design and decreased with decreasing fabric density. The introduction of pillar stitch resulted in an increased fabric thickness and weight compared to the same fabric without pillar stitch (Table 2). The twists in the jacket resulted in a disc with slightly thicker central areas on both cranial and caudal surfaces. As a result, both jackets with pillar stitch fabrics had a significant thicker knot of approximately 0.2 mm at cranial and caudal sides of the device and overall disc height caused by the twisting assembly method (Fig. 3).

To assess which textile structure is more suitable to facilitate osseointegration by cell infiltration, the pore sizes of the different textile structures were measured (Table 2). The pore sizes were mostly influenced by the lapping design, being highest for 1 × 1 lapping, followed by 1 × 1 with pillar stich, 2 × 1 and 2 × 1 with pillar stitch. The reduction in fabric density also gave rise to larger pore sizes for the same textile structure.

Fabric mechanical properties

Abrasion resistance (number of rubs needed until loop damage) was only influenced by the introduction of a pillar stitch, and not by the lapping design or change in fabric density (Table 2). On the other hand, bursting strength (force required for loop rupture) increased for the 2 × 1 lapping design compared to 1 × 1 and when introducing a pillar stitch (Table 2). Overall, the effect of the pillar stitch on the bursting strength was significant compared to the effect of the lapping design.

Device evaluation: swelling and mechanical integrity

Effect of knitting lapping design

Only the combination of the 2 × 1 lapping design with pillar stitch decreased the swelling capacity significantly compared to the other stitch patterns (Fig. 4). Restricting the swelling results in an osmotic internal pressure required to withstand compressive forces. When looking at the compressive properties, it can be seen that all textile structures were able to withstand more than the physiological load of 75 N (Fig. 4) [11, 12]. However, using the 2 × 1 lapping, either with or without pillar stitch, increased both the ultimate load as well as the stiffness of the bioAID above peak and impact loads reported to range between 100 and 1200 N and physiological stiffness of 500 N/mm [11, 13–15]. For the ultimate load, this was only statistically significant for the 2 × 1 with pillar stitch. No macroscopical damage of the fiber

Table 2 Fabric properties for the 4 different textile structures with either fabric density of 10 stitch/cm or 8 stitch/cm

	Fabric thickness (mm)	Fabric weight (g/m²)	Fabric pore size (μm)	Abrasion resistance (cycles)	Burst strength (MPa)
	Density of 10 stitch/cm				
1 × 1	0.35 ± 0.005	91 ± 0.88	1150 ± 25	50,000 ± 2083	1.25 ± 0.07
1 × 1 + pillar stitch	0.47 ± 0.004	154 ± 0.57	940 ± 50	55,000 ± 2291	1.68 ± 0.10
2 × 1	0.53 ± 0.004	128 ± 0.72	730 ± 35	50,000 ± 2083	1.46 ± 0.10
2 × 1 + pillar stitch	0.80 ± 0.005	176 ± 1.2	400 ± 50	60,000 ± 2500	1.84 ± 0.11
	Density of 8 stitch/cm				
2 × 1	0.48 ± 0.006	110 ± 0.83	860 ± 25	50,000 ± 2083	1.14 ± 0.05
2 × 1 + pillar stitch	0.61 ± 0.005	158 ± 0.93	540 ± 40	60,000 ± 2500	1.60 ± 0.09
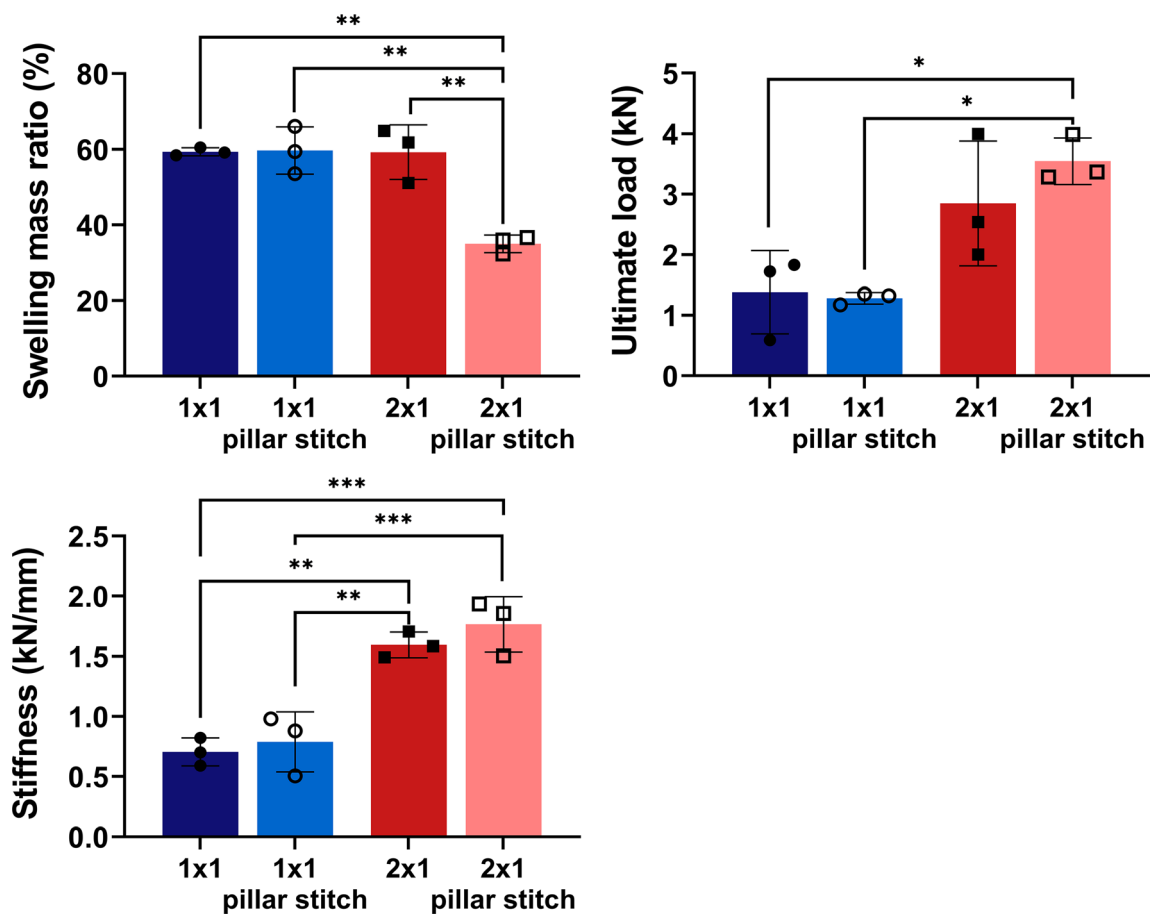
Figure 4 Swelling mass ratio, compressive ultimate load and compressive stiffness (mean ± SD) of each fiber jacket design in human prototypes. One-way ANOVA (*$p < 0.05$, **$p < 0.01$, ***$p < 0.001$).

jacket was observed after the test, bioAIDs failed due to cracking of the hydrogel.

Effect of the number of jacket layers

Based on the results of the different textile structures, it was concluded that both 2 × 1 lapping with and without pillar stitch seemed to be best for ensuring safety under physiological compressive loads of the bioAID. Therefore, these two textile structures were assessed to determine the number of layers for optimal functioning of the full device. No significant effect could be observed between the different knits and number of layers used, and all groups were able to withstand the physiological load of 75 N (Fig. 5) [11, 12]. No macroscopical damage of the jacket was observed after the test.

Discussion

In the previous design, the integrity of the fiber jacket using single yarn weft-knitting technique was not full proof and could have become compromised, especially since it is often exposed to sharp bony protrusions and sharp surgical tools during implantation [6]. Using warp-knitting as a textile structure reduces the risk of disintegration upon yarn damage since it is produced from multiple yarns. Therefore, the objective of this study was to investigate several warp-knitted textile patterns for the fabrication of a novel biomimetic disc replacement device.

One of the most important requirements of the fiber jacket is limiting the swelling of the hydrogel to replicate the semi-constrained motion characteristics seen in a natural disc [16]. The semi-constrained motion, where small deformations are easily allowed by the soft hydrogel, while larger deformations are resisted by the tensile strong jacket, have been assessed in another study [17]. In this research, all devices had a swelling capacity of 60% or less
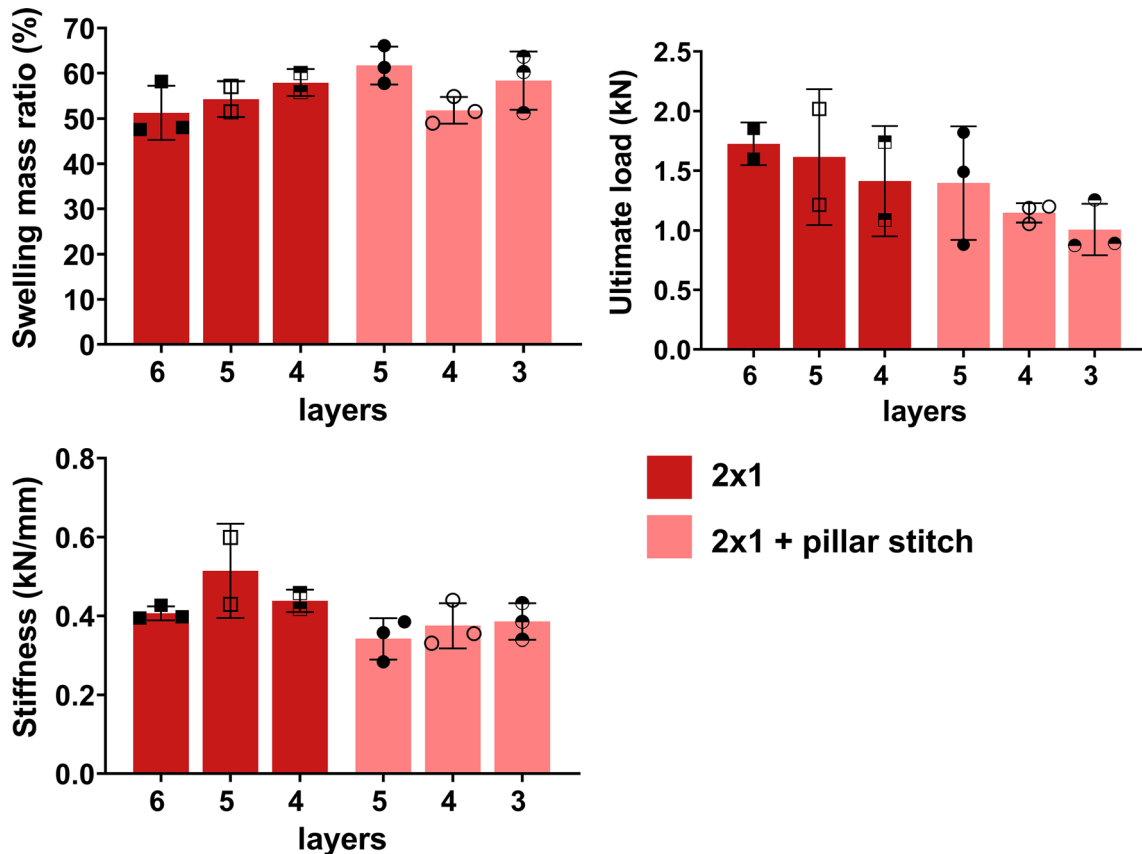

Figure 5 Swelling mass ratio, compressive ultimate load and compressive stiffness (mean ± SD) and corresponding number of layers of 2 × 1 and 2 × 1 + pillar stitch structures in canine prototypes.

compared to the mass immediately after preparation. Previous results (data not shown) have shown that the isolated hydrogel can swell up to double its initial weight when swollen unconstrained [18]. This indicates that all the different textile groups are capable of restricting the swelling of the hydrogel to create an internal pressure that can withstand physiological compressive forces. Only the combination of 2 × 1 lapping design with a pillar stitch resulted in a significantly lower swelling. This might be related to the pillar stitch, resulting in a reduced stretchability. When reducing the density to 8 stitch/cm, this effect becomes nonapparent.

This difference in swelling capacity did not affect the ultimate compressive load and stiffness of the complete device, which was most influenced by the lapping design. The 2 × 1 lapping design showed a significantly higher stiffness and ultimate load, and no effect of the pillar stitch was visible. This can be explained by the fact that the underlap is longer and has a flatter course, making it less elastic in the transverse direction compared to the 1 × 1 lapping structure [19]. The lack of influence of introducing a pillar stitch can be explained by the fact that there is no lateral connection but only a connection with the other binding elements of the lapping design, increasing the stability only in the longitudinal (and radial) direction [20]. Although loads in normal daily life that are being transferred through the intervertebral disc all have a compressive component, these findings cannot be extrapolated to all different loading modes that act on a spinal segment. Therefore, additional studies that assess multiple loading modes and investigate the effect on the kinematics of the spine are required.

Although the function of UHMWPE membrane is to contain the hydrogel, it is loose and does not limit it from swelling. Thus, it was relevant to assess if the fiber jacket could withstand the hydrogel's swelling pressure without yarn rupture. As can be seen from the bursting strength data, all textile patterns only failed above the previously measured hydrogel swelling pressure tested in a rigidly confined compression setup of 1 MPa [18]. Also being above the physiological internal pressures measured for natural nucleus pulposus that ranges between 0.3 and 1 MPa [12, 21–23]. This is also consistent with the results of the swelling and compression test of the full device, where no macroscopical damage of the fiber jacket was observed.

To ensure longevity of the device, the fiber jacket should be wear resistant as the layers of the fiber jacket are not restricted from moving relative to each other. To assess the wear performance of the different textile patterns, an abrasion test was performed to give insight into the number of cycles needed before a loop is damaged, which could potentially weaken the fiber jacket. The differences in abrasion resistance between the different textile structures were small, and only the introduction of a pillar stitch in the 2 × 1 lapping design resulted in a significantly increased abrasion resistance. This indicates that the yarn and its mechanical properties play the largest role in the jacket's wear performance. It is known that UHMWPE yarns have an extremely high wear resistance, represented by its high abrasion resistance and flex life (> 100 000 cycles) [7, 24]. This indicates that the risk of yarn rupture causing weakening of the complete fiber jacket is assumed to be minimal for all the textile structures that were investigated. This study did not include assessment of wear debris, which can trigger an inflammatory response that could lead to aseptic loosening and prosthesis failure [24]. Therefore, further work is needed to establish this risk of wear debris, especially since in the current design multiple layers of UHMWPE textile are used that can rub against each other, increasing the risk of creating wear particles. However, as no yarn rupture occurred one could assume that this is not of considerable volume. The risk is even further reduced after bone has grown into multiple layers of the fiber jacket, limiting motions that could cause wear. In addition, the durability, fatigue and creep properties of the jacket and full device should also be assessed to get a more complete picture of the bioAIDs longevity.

Another important aspect that should be considered when designing the fiber jacket is that the surface directly interfacing the vertebral bodies should facilitate osseointegration, known to be one of the most critical parameters influencing clinical success [25–27]. In this study, based on the structural properties, it was assessed if the pore size of each textile structure would allow cell infiltration. For both stitch densities, only the 2 × 1 with pillar stitch design was within the optimal range of 100–600 μm [28–33]. It should however be noted that by introducing multiple layers, the total porosity of the jacket is affected and likely reduced. It was therefore assumed that also the 2 × 1 lapping design could be a

suitable surface for cell infiltration. Besides structural properties, chemical and physical characteristics will also influence the osseointegration of the device. UHMWPE is known to be inert and hydrophobic, and thus unsuitable for cells to adhere to [34]. Hence, to improve the osseointegration potential of the bioAID, surface modifications, such as plasma treatment or hydroxyapatite coatings, which improve bioactivity should be assessed in future research [35].

The fiber jacket should behave as a homogeneous structure that covers the hydrogel and endplate such that it behaves as one integrated unit similar to a natural IVD. This can be either achieved by increasing the stitch density or by wrapping the hydrogel and endplate in multiple layers. Based on the fabric mechanical properties, especially the 2×1 and 2×1 with pillar stitch of both the 8 stitch/cm and 10 stitch/cm samples demonstrated to be suitable for functioning of the bioAID. However, an advantage of the 8 stitch/cm fabrics is that it can be produced on more commonly available textile machines, improving the manufacturing capabilities and quality control. It was also expected that decreasing the stitch density from 10 stitch/cm to 8 stitch/cm would lead to a reduced compressive strength of the complete device. Thus, although the 10 stitch/cm 1×1 lapping prototypes resembled the natural stiffness better, it was decided to continue with the 2×1 and 2×1 with pillar stitch and prioritize manufacturing feasibility and a higher failure load to ensure structural integrity under reported impact loads of 100–1200 N [11, 13–15]. Therefore, the effect of layers on functioning of the bioAID for the 2×1 and 2×1 with pillar stitch textile structures was investigated with 8 stitch/cm density structures. The results of the 8 stitch/cm samples also confirmed this decrease in stiffness, showing stiffness ranging between 400 and 500 N/mm.

No statistical differences in swelling and mechanical characteristics were found between samples with different layers or stich densities, making the structural parameters of the bioAID after assembly an important consideration for choosing the most optimal jacket configuration. By introducing a pillar stitch, the textile construct becomes denser and heavier because of the higher yarn consumption in the underlap. As a result, the twists in the 2×1 with pillar stitch jacket resulted in a disc with a significantly thicker center part on both cranial and caudal sides compared to the 2×1 samples. This was considered to be a disadvantage for the implantation of the device, increasing the risk of over distracting the disc space. Moreover, the 2×1 textile structure with pillar stitch has a fabric thickness that with only 3 layers already results in a final thickness of approximately 4 mm when unswollen. The optimal height of the device should be within the physiological height range of the IVD of the cervical spine, being between 4 and 6 mm [36–38]. Therefore, the 2×1 lapping design was considered to be most optimal based on all discussed parameters. To reduce the need of vertebral distraction during implantation, four layers was hypothesized to be most optimal.

This study was focused on the effect of fabric properties within a novel cervical disc replacement device. While this study varied in testing human and canine prototypes (as preparation for animal trials), complicating mutual comparisons, it was still useful for determining the optimal fiber jacket configuration. It would, however, be valuable to investigate the complex interplay of the textile structure, geometry and yarn properties in future studies. In addition, it should be noted that the current device is still a prototype, requiring multiple manual assembly steps that can give rise to variabilities and suboptimal characteristics such as the knot formation due to the jacket twisting. In the future, it would be desirable to set up a more automated assembly procedure to rule out these effects. Taken together, these findings suggest that using 4 layers of the 2×1 lapping structure is the most optimal configuration for functioning of the bioAID and future studies.

Acknowledgements

Author's contributions

CJ, AA, SG, SJ and KI conceived and designed the study. CJ and AA executed the experimental work and obtained all the data presented in this publication. Critical revising of the article was done by all authors. Approval of the submitted version was given by all authors.

Data and code availability

Data are available upon reasonable request.

Declarations

References

[1] Webb R, Brammah T, Lunt M, Urwin M, Allison T, Symmons D (2003) Prevalence and predictors of intense, chronic, and disabling neck and back pain in the Uk general population. Spine (Phila Pa 1976) 28(11):1195–1202

[2] Smeathers JE, Joanes DN (1988) Lumbar intervertebral joints: a comparison between fresh and thawed specimens. J Biomech 21(5):425–433

[3] Shim CS et al (2007) CHARITI versus ProDisc: a comparative study of a minimum 3-year follow-up. Spine (Phila Pa 1976) 32(9):1012–1018

[4] Rousseau MA, Bradford DS, Bertagnoli R, Hu SS, Lotz JC (2006) Disc arthroplasty design influences intervertebral kinematics and facet forces. Spine J 6:258–266

[5] C. A. M. Jacobs, C. J. Siepe, and K. Ito, "Viscoelastic cervical total disc replacement devices: Design concepts," Spine Journal, vol. 20, no. 12. Elsevier, pp. 1911–1924, Aug-2020.

[6] Van Den Broek PR (2012) Development of a biomimetic artificial intervertebral disc. Eindhoven University of Technology

[7] Kirschbaum R, van Dingenen JLJ (1989) Advances in gel-spinning technology and Dyneema fiber applications Integration of fundamental polymer science and technology, vol 3. Springer, Dordrecht, pp. 178 198

[8] van den Broek PR, Huyghe JM, Wilson W, Ito K (2012) Design of next generation total disk replacements. J Biomech 45(1):134–140

[9] Elmogahzy YE (2019) Engineering textiles: integrating the design and manufacture of textile products. Eng. Text. Integr. Des. Manuf. Text. Prod., pp 1–448

[10] Ghazanfari S, Werner A, Ghazanfari S, Weaver JC, Smit TH (2018) Morphogenesis of aligned collagen fibers in the annulus fibrosus: mammals versus avians. Biochem Biophys Res Commun 503(2):1168–1173

[11] Moroney SP, Schultz AB, Miller JAA (1988) Analysis and measurement of neck loads. J Orthop Res 6(5):713–720

[12] Arshad R, Schmidt H, El-Rich M, Moglo K (2022) Sensitivity of the cervical disc loads, translations, intradiscal pressure, and muscle activity due to segmental mass, disc stiffness, and muscle strength in an upright neutral posture. Front Bioeng Biotechnol 10(April):1–11

[13] Moroney SP, Schultz AB, Miller AAJ, Andersson GBJ (1988) Load-displacement properties of lower cervical spine motion segments. J Biomech 21(9):769–779

[14] Yoganandan N, Pintar FA, Zhang J, Baisden JL (2009) Physical properties of the human head: mass, center of gravity and moment of inertia. J Biomech 42(9):1177–1192

[15] Funk JR, Cormier JM, Bain CE, Guzman H, Bonugli E, Manoogian SJ (2011) Head and neck loading in everyday and vigorous activities. Ann Biomed Eng 39(2):766–776

[16] Bogduk N, Mercer S (2000) Biomechanics of the cervical spine. I: normal kinematics. Clin Biomech 15:633–648

[17] Jacobs CAM et al (2022) Biomechanical evaluation of a novel biomimetic artificial intervertebral disc in canine cervical cadaveric spines. JOR Spine 1251:1–10

[18] Jacobs C, Wijlaars M, Harries M, Ito K, Kock L 2019 () A novel cervical biomimetic artificial intervertebral disc: a mechanical analysis. Eur Soc Biomech, p 1

[19] Anbumani N (2007) Knitting Fundamentals, Machines, Structures and developments. New Age International

[20] Kyosev Y (2019) Warp knitted fabrics construction. Warp Knitt. Fabr. Constr., pp 1–302

[21] Frost B, Camarero-Espinosa S, Foster E (2019) Materials for the spine: anatomy, problems, and solutions. Materials (Basel) 12(2):253

[22] Pospiech J, Stolke D, Wilke HJ, Claes LE (1999) Intradiscal pressure recordings in the cervical spine. Neurosurgery 44(2):379–385

[23] Wang K, Deng Z, Wang H, Li Z, Zhan H, Niu W (2017) influence of variations in stiffness of cervical ligaments on C5–C6 segment. J Mech Behav Biomed Mater 72(1):129–137

[24] Werner JH, Rosenberg JH, Keeley KL, Agrawal DK (2018) Immunobiology of periprosthetic inflammation and pain following ultra-high-molecular-weight-polyethylene wear debris in the lumbar spine. Exp Rev Clin Immunol. Taylor and Francis Ltd.

[25] Lee CK, Goel VK (2004) Artificial disc prosthesis: design concepts and criteria. Spine J 4(6):S209–S218

[26] Eijkelkamp MF, Huyghe JM, van Donkelaar CC, van Horn JR, Veldhuizen AG, Verkerke GJ (2001) Requirements for an artificial intervertebral disc. Int J Artif Organs 24(5):311–321

[27] Kienapfel H, Sprey C, Wilke A, Griss P (1999) Implant fixation by bone ingrowth. J Arthroplasty 14(3):355–368

[28] Li G et al (2016) In vitro and in vivo study of additive manufactured porous Ti6Al4V scaffolds for repairing bone defects. Sci Rep 6:1–11

[29] Karageorgiou V, Kaplan D (2005) Porosity of 3D biomaterial scaffolds and osteogenesis. Biomaterials 26(27):5474–5491

[30] Taniguchi N et al (2016) Effect of pore size on bone ingrowth into porous titanium implants fabricated by additive manufacturing: an in vivo experiment. Mater Sci Eng C Mater Biol Appl 59:690–701

[31] Chen Z et al (2020) Influence of the pore size and porosity of selective laser melted Ti6Al4V ELI porous scaffold on cell proliferation, osteogenesis and bone ingrowth. Mater Sci Eng C Mater Biol Appl 106:1–13

[32] Augustin J et al (2022) Effect of pore size on tissue ingrowth and osteoconductivity in biodegradable Mg alloy scaffolds. J. Appl. Biomater. Funct. Mater. 20:1–18

[33] Li W et al (2022) Pore size of 3D-printed polycaprolactone/polyethylene glycol/hydroxyapatite scaffolds affects bone regeneration by modulating macrophage polarization and the foreign body response. ACS Appl Mater Interfaces 14(18):20693–20707

[34] Vaishya R, Agarwal AK, Tiwari M, Vaish A, Vijay V, Nigam Y (2018) Medical textiles in orthopedics: an overview. J Clin Orthop Trauma 9S:S26–S33

[35] Jacobs CAM, Cramer EEA, Dias AA, Smelt H, Hofmann S, Ito K (2022) "Surface modifications to promote the osteoconductivity of ultra-high-molecular-weight-polyethylene fabrics for a novel biomimetic artificial disc prosthesis: an in vitro study. J Biomed Mater Res Part B Appl Biomater 111:1–11

[36] Frobin W, Leivseth G, Biggemann M, Brinckmann P (2002) Vertebral height, disc height, posteroanterior displacement and dens-atlas gap in the cervical spine: Precision measurement protocol and normal data. Clin Biomech 17(6):423–431

[37] Busscher I, Ploegmakers JJW, Verkerke GJ, Veldhuizen AG (2010) Comparative anatomical dimensions of the complete human and porcine spine. Eur Spine J 19(7):1104–1114

[38] Anderst W, Donaldson W, Lee J, Kang J (2016) Cervical spine disc deformation during in vivo three-dimensional head movements. Ann Biomed Eng 44(5):1598–1612

Springer